Optics and Photonics Journal, 2022, 12, 215-224
https://www.scirp.org/journal/opj
ISSN Online: 2160-889X
ISSN Print: 2160-8881

Improved Interface of Encapsulating Sm-Doped TiO_2 Thin Films/RuO_2 Schottky Diodes for a Junction Spectropy Measurement

Mariko Murayama[1,2*], Yuri Tamamoto[1], Yingda Qian[1], Asuka Ishizawa[1], Simon Hammersley[3], Iain F. Crowe[3], Shuji Komuro[2], Xinwei Zhao[1]

[1]Department of Physics, Tokyo University of Science, Tokyo, Japan
[2]Research Institute of Industrial Technology, Toyo University, Saitama, Japan
[3]Photon Science Institute and School of Electrical and Electronic Engineering, University of Manchester, Manchester, UK
Email: *mariko.murayama@rs.tus.ac.jp

How to cite this paper: Murayama, M., Tamamoto, Y., Qian, Y.D., Ishizawa, A., Hammersley, S., Crowe, I.F., Komuro, S. and Zhao, X.W. (2022) Improved Interface of Encapsulating Sm-Doped TiO_2 Thin Films/RuO_2 Schottky Diodes for a Junction Spectropy Measurement. *Optics and Photonics Journal*, **12**, 215-224.
https://doi.org/10.4236/opj.2022.1210016

Received: September 29, 2022
Accepted: October 28, 2022
Published: October 31, 2022

Abstract

The excitation process of rare-earth ions in oxide semiconductors for optical emission is thought to be related to defect levels within the band-gap of the host material. In order to improve understanding of the role defect levels play in the energy transfer process, junction spectroscopy techniques can be used to investigate the electrically active emission centres. It has been reported that TiO_2 is sensitive to humidity at low temperatures, such as those employed when conducting junction spectroscopy measurements. However, there are not many discussions how to prevent this effect and to improve the quality of measurements. After optimization of samples such as fabrication of flat surface and encupsulant for preventing external effect, temperature dependent-capacitance measurements (C-T) were carried out to characterise shallow traps formed within TiO_2 band-gap. TiO_2 and Sm-doped TiO_2 thin films were deposited on $SrTiO_3$(100) templates by laser ablaton and rectifying Ruthenium Oxide Schottky diodes deposited on the TiO_2 surface by laser ablation. A Sm or Sm-related shallow trap was observed in the Arrhenius plot of TiO_2:Sm. In this paper, we show the optimized sample fabrication/preparation process that stabilizes the junction spectroscopy measurements, even in the presence of humidity and we present initial results obtained on samples using these optimized processing techniques.

Keywords

Rare Earth, TiO_2, Photoluminescence, Junction Spectroscopy

1. Introduction

Rare-earth (RE)-doped wide band-gap semiconductors exhibit sharp and intense emission covering a wide (visible to near-IR) spectral range [1] [2] [3] [4] [5]. The direct (resonant) absorption cross-section of RE ions tends to be very small (and the resulting emission relatively weak) but (orders of magnitude more) intense emission can result when the RE ions are indirectly excited, via the host material. The $4f$ electronic-dipole transition in RE ions is generally forbidden, with very weak (oscillator strength, $f < 10^{-6}$) magnetic-dipole, and electric-quadrupole, type transitions [6] [7]. The spin-orbit interaction lowers the degeneracy of the RE ions to the order of 10^3 cm^{-1} and splits the $^{(2S+1)}L$-terms into multiplets, where S is spin and L is orbital momenta. Each multiplet is many-fold degenerate, the lowering of which results from external effects such as local (crystal) electric or magnetic fields.

It is thought that this improvement in emission intensity is the result of defect levels, within the band-gap of the host material, introduced by, and/or strongly coupled to, the RE species within the host crystal lattice [8]. In order to improve our understanding of the role that these energetically deep defect levels play in the energy transfer process, junction techniques, such as deep level transient spectroscopy (DLTS) and admittance spectroscopy can be used to investigate how such levels interact with the emission centres [9]-[14]. In order to do this, it is essential to fabricate either p-n or Schottky-type junctions with good rectification/low leakage currents [15] [16] [17] [18]. In addition, especially for semi-insulating materials such as Titania (TiO_2) sample quality (e.g. grain boundaries) and conductivity is key to improving practical devices [19]. In this paper, TiO_2 is selected as a host material for Samarium (Sm), one of the rare-earths exhibiting red and infrared emission.

To this end, here we report C-T analysis, evaluating sample quality with respect to shallow defects in Sm-doped TiO_2 thin films. Specifics of the device behaviour when cycling the sample temperature and vacuum pressures are discussed and further ways to optimize device quality/improve device longevity and stability under these conditions is also considered.

2. Experimental

Anatase-phase TiO_2 thin films with and without Sm_2O_3 (1.0 wt%) were fabricated on $SrTiO_3$(100) substrates (7 - 10 × 10^{-2} Ω·cm) by laser ablation. Note that $SrTiO_3$ substrate was used as the backside Ohmic contact for the samples. The growth rate during deposition was carefully controlled by maintaining a target-substrate gap between 45 and 60 mm, which we have found previously to be optimum. A ceramic target was ablated by the third harmonic line of a neodymium yttrium aluminium garnet (Nd:YAG) laser (355 nm) with a laser fluence of 1 J/cm^2. The atomic density of Sm dopant in the target was calculated to be 1.1 × 10^{20} cm^{-3} and the thickness of the resulting thin films was approximately 900 nm. Sample growth is also determined by oxygen pressure in the chamber,

which we have previously determined to be optimum at 1.5×10^{-2} Torr. Detailed information regarding the influence of oxygen pressure on TiO_2 crystal structure/quality was reported elsewhere [20]. The fabricated samples were annealed at 500˚C for 1 h in an O_2 atmosphere in order to activate the Sm^{3+} ions and induce the formation of nanometer-sized TiO_2 crystals. The Schottky barrier diodes (1 mm in diameter) were formed on the TiO_2:Sm/$SrTiO_3$ samples by laser ablating RuO_2. Note that RuO_2 was selected for forming the rectifying junction in n-type TiO_2/TiO_2:Sm because of its large work function, crystal (rutile) structure and thermal resistivity [21] [22].

Structural characterization was determined by x-ray diffraction (XRD), which confirmed that the samples were anatase-phase. Also, crystalline grain size was derived from a Scherrer analysis of the XRD peak width. Morphological (imaging) analysis was carried out with a SUPRA40, Carl Zeiss Scanning electron microscope (SEM). Current-Voltage (I-V) characteristics were evaluated using a 4140B pA meter/DC voltage source (HP). Capacitance-Temperature (C-T) measurements were conducted using a 4192A LF Impedance Analyzer (HP), in order to evaluate the shallow defect levels formed in the TiO_2 host. During these measurements, a fixed reverse bias voltage of 0.25 V was used throughout.

3. Result and Discussion

3.1. Optimization of Sample Fabrication/Preparation Process for Junction Spectroscopy

Figure 1(a) shows the surface morphology (via SEM) of TiO_2:Sm sample fabricated using a target-substrate distance of 45 mm. Droplets with a large range of sizes (from sub-100 to ~800 nm) can be seen in the image. For the sample fabricated with the larger target-substrate distance of 60 mm, the slower growth rate helps achieve a smoother surface morphology. A smaller number of these droplets is apparent on TiO_2:Sm sample prepared with 60 mm separation compared to the sample fabricated with 45 mm separation as shown in **Figure 1(b)**. It is suggested that the reduction of these droplets is caused by the lower kinetic energy arising from the slower growth rate when the target-substrate distance is larger [23] [24]. Crystalline grain size of these samples is derived from a Scherrer analysis of the full width at half maximum (FWHM) of XRD peaks. "Grain size" of the sample prepared with 60 mm separation was approximately 55 nm, whereas the grain size was about 40 nm for the fabricated with 45 mm separation sample. This suggests that the sample fabricated with 60 mm separation has many pure TiO_2 and Sm_2O_3 crystals which can be grown larger by annealing. On the other hand, the sample prepared with 45 mm separation, the thin film has droplets, clusters, and pure crystals. The droplets and clusters are not able to grow with heating so that its grain size was smaller than the sample prepared with longer separation. Larger grain size attributes to decrease in band-gap energy and resistivity due to reduced scattering centers at the grain boundaries [25] [26]. The films fabricated with 60 mm separation (and fewer droplets) were

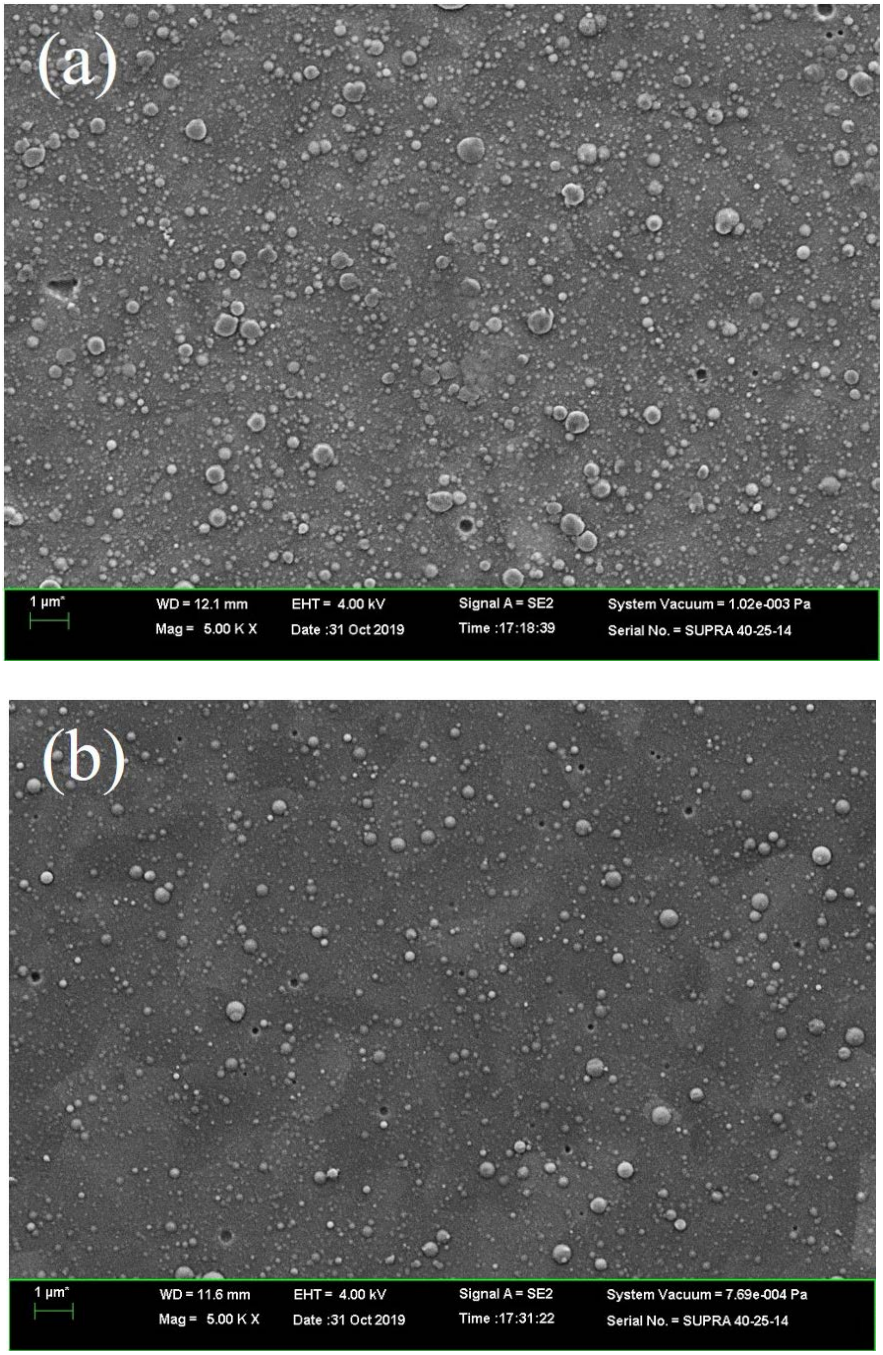

Figure 1. SEM images of TiO_2:Sm samples fabricated with the target-substrate distance d = (a) 45 mm and (b) 60 mm.

also found to exhibit improved I-V and C-V characteristics, although, in spite of this, they were still found to be relatively unstable at low temperature.

The sample showed reasonably small leakage current of 4.51×10^{-5} A at −2 V for junction spectroscopy measurements. Then, the cryostat was pumped up and cooled down to 100 K for obtaining I-V characteristics of the sample at low temperature. The rectifying Schottky junction disappears at low temperature which is more likely the Ohmic junction characteristic. This unstable electrical

property occurs every time samples are in a cooled cryostat. The exact cause of this remains uncertain but we suspect, (as a result of the sensitivity of TiO_2 to humidity; TiO_2 has been applied to hydrogen-related devices such as photocatalysis and hydrogen sensors because of its high sensitivity to humidity [27] [28] [29]) this is the result of humidity, which can lead to the formation of shallow surface states. This can cause dificulties, even when carrying out measurements at low temperature. Komuro *et al.* reported that the broad PL peak at 530 nm from TiO_2:Er_2O_3 was observed at low temperature and suppressed luminescence from Er^{3+} ions which induced by both the H_2O adsorption and the reduction process of TiO_2 to Ti_2O_3 by UV illumination [30]. Also, authors noted careful protection of the sample surface against humidity and UV exposure was essential to avoid electrical degradation. To prevent these effects, the samples were encapsulated with dried photoresist. The samples with positive resist were irradiated by a Xe lamp through a mask with 1.0 mm diameter circles. Then, Au thin films were manufactured using thermal evaporation on the samples. The samples were washed in organic solvent for a lift-off process on Au thin films. Finally, for making electrode contacts, the samples with negative resist were illuminated by a Xe lamp through a mask with 0.5 mm diameter circles. With encapsulant, IV characteristic of the rectifying Schottky junction is preserved at low temperature. This process worked well for producing "low temperature-resistant" (stable) samples.

3.2. Temperature Dependent-Capacitance Measurements for Estimation of Shallow Traps

Figure 2(a) demonstrates temperature-dependent capacitance (C-T) of TiO_2 sample with photoresist coating at −0.25 V in the temperature range 150 to 400 K. Capacitance increased from 128 to 240 pF with increasing temperature. Although the data appears to indicate a broad peak, further increases in temperature were not possible to confirm this. In contrast, a broad peak around 350 K was observed in the C-T data for Sm-doped TiO_2 as illustrated in **Figure 2(b)**. Note that an anomalous point around 325 K is a fluctuation during the measurement and it is not related to any defect states. TiO_2:Sm sample exhibited a much larger capacitance, also with an approximate factor 2 increase, from 360 to 700 pF with increasing temperature. This result indicates that doping Sm increased the carrier concentration in the TiO_2. The broad peak at 350 K for TiO_2:Sm suggests the presence of an energetically shallow defect level is induced by the presence of Sm in TiO_2.

C-T curves of **Figure 3(a)** TiO_2 and **Figure 3(b)** TiO_2:Sm were replotted as an Arrhenius plot, ($\ln C$ against 1/kT) in order to evaluate the shallow levels formed in TiO_2 host and demonstrated in **Figure 3**. This slope(s) associated with this data indicates the presence of several shallow donor activation levels for both samples. However, the presence of an inverted slope for the TiO_2:Sm sample, especially given the applied bias, possibly indicates charge carrier type reversal in otherwise n-type TiO_2, suggestive of the presence of a shallow acceptor level

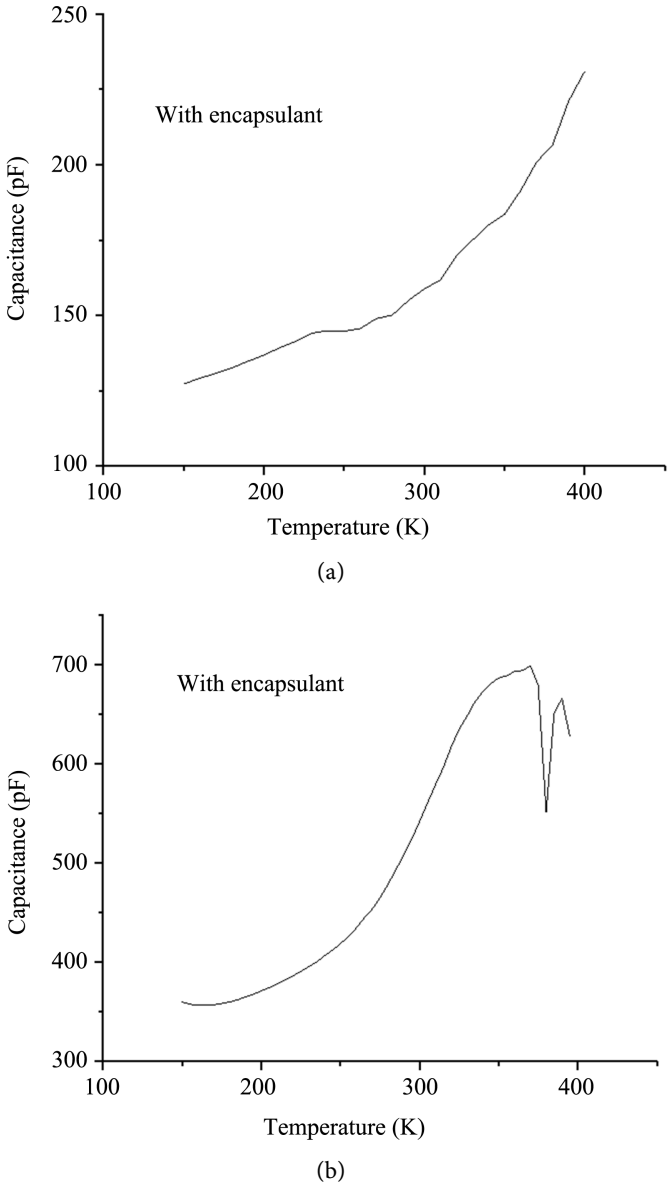

Figure 2. Temperature dependence of capacitance of (a) TiO_2 and (b) TiO_2:Sm thin films in the temperature range 150 - 400 K with fixed bias voltage of −0.25 V.

formed in this sample. Activation energies, determined from the fitting of these slopes are shown in **Table 1**. From the Arrhenius data, the activation energy of the shallow acceptor level which is described as "Highest T" in **Figure 3(b)**, E_1 of TiO_2:Sm has been determined to be 0.039 ± 0.009 eV. From the range of "High T", in **Figure 3(a)** and **Figure 3(b)**, E_1 of TiO_2 and E_2 of TiO_2:Sm are evaluated as 0.035 ± 0.002 eV and 0.041 ± 0.001 eV. Finally, in the "Low T" range, E_2 of TiO_2 and E_3 of TiO_2:Sm are determined as 0.0047 ± 0.0018 eV and 0.0055 ± 0.0045 eV. These results suggest that there is existence of couple of shallow donor levels formed around 33 to 42 meV and 3.0 to 10 meV in TiO_2 and TiO_2:Sm samples. Also it is suggestive that the positive gradient shown in **Figure 3(b)** is a shallow acceptor level formed around 30 to 48 meV in TiO_2:Sm.

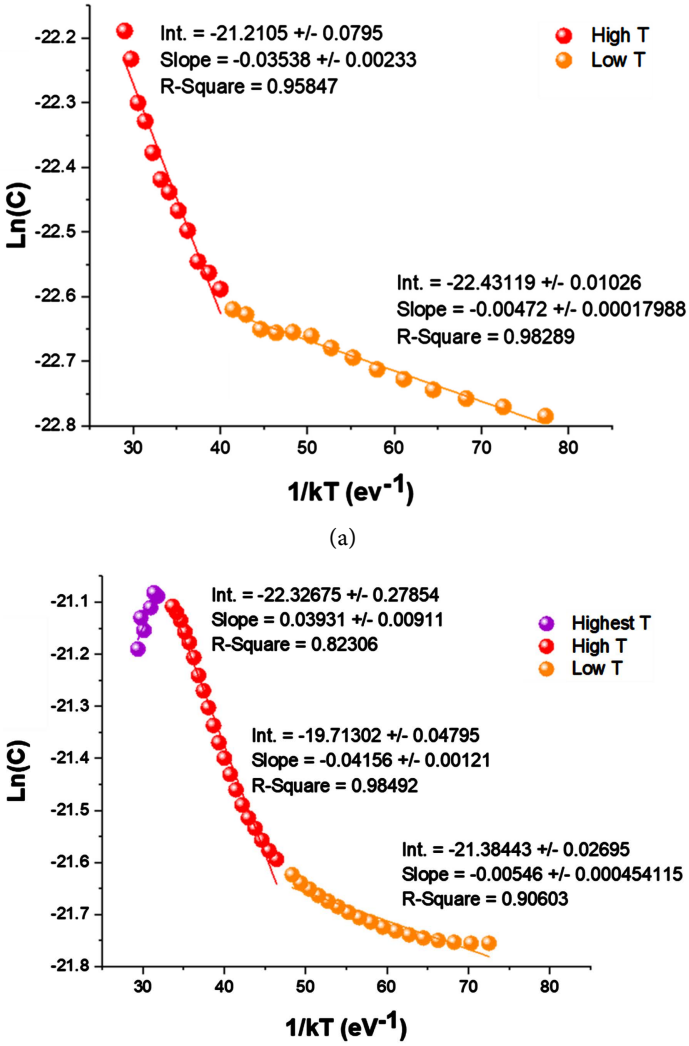

Figure 3. C-T Arrhenius plots of $\ln(C)$ against $1/kT$ (a) TiO_2 and (b) TiO_2:Sm.

Table 1. Activation energy calculated from Arrhenius data of TiO_2 and TiO_2:Sm.

TiO_2	E_A (meV)	TiO_2:Sm	E_A (meV)
E_1	35.4 ± 2.3	E_1	39.3 ± 9.1
E_2	4.72 ± 0.18	E_2	41.5 ± 1.2
	-	E_3	5.46 ± 0.45

4. Conclusions

Anatase-TiO_2:Sm thin films were fabricated on $SrTiO_3$(100) using laser ablation with two different target-substrate distances, 45 mm and 60 mm. The morphology of TiO_2:Sm samples were observed by SEM. Samples with 60 mm separation showed less droplets and clusters on the surface than those with d = 45 mm, which was also correlated with improved electronic properties. The room temperature I-V characteristics of the rectifying Schottky junction appear to become

more Ohmic-like as the temperature is decreased. It has been reported that TiO_2 is sensitive to hydrogen at lower temperatures, however enough discussions have not been done especially about contacts and fabrication process for electrical measurements. Encapsulation of samples with photoresist was found to stabilize the TiO_2 at lower temperatures. This makes TiO_2 junction spectroscopy possible for these samples and the data obtained reproducible.

Temperature dependent-capacitance (C-T) measurements were carried out in the range 150 - 400 K with fixed bias voltage of −0.25 V. The C-T curve of the TiO_2:Sm sample revealed a broad peak around 350 K, whereas for TiO_2, a gentle slope was observed. C-T data were converted to Arrhenius plots, ($\ln(C)$ against $1/kT$) to determine the activation energy of traps. One acceptor or compensating level and 2 donor levels were observed in the Sm-doped sample, with activation energies of 39.3 ± 9.1, 41.5 ± 1.2, 5.46 ± 0.45 meV, respectively. In the Sm free TiO_2 sample, just 2 donor levels were observed, with activation energies of 35.4 ± 2.3 and 4.72 ± 0.18 meV. It can be assumed that doping Sm formed shallow acceptor or possibly compensating trap in TiO_2 host.

In this paper, we showed how to optimize the sample fabrication process to stabilize TiO_2 at lower temperatures, facilitating junction spectroscopy measurements to prevent degradation by hydrogen. This has allowed us to discern subtle differences in the electronic properties of charge carrier traps, as a result of doping TiO_2 with Sm. Doping with Sm appears to introduce a shallow acceptor level, which was not observed in the undoped TiO_2.

Acknowledgements

The authors express their gratitude to Prof Matthew P. Halsall, Dr Ian D. Hawkins, Dr Vladimir P. Markevich and Prof Tony R. Peaker of Photon Science Institute, The School of Electronic Engineering, University of Manchester for their technical support and advice. Also, authors would like to thank Dr Masashi Ishii of National Institute for Materials Science for fruitful discussions, advice, and support.

Conflicts of Interest

The authors have no conflicts of interest.

References

[1] Murayama, M., Yoda, K., Komuro, S., Crowe, I.F. and Zhao, X. (2019) Effect of Al Co-Doping on the Luminescence Properties of Nd^{3+}-Doped TiO_2 Thin Films. *Journal of Luminescence*, **216**, Article ID: 116656. https://doi.org/10.1016/j.jlumin.2019.116656

[2] Murayama, M., Yoda, K., Shiraishi, K., Crowe, I.F., Komuro, S. and Zhao, X. (2019) Photoluminescence Enhancement and Change in the Second Nearest Neighbor Distance of Sm-Doped TiO_2 Thin Films. *Physica Status Solidi B*, **256**, Article ID: 1800522. https://doi.org/10.1002/pssb.201800522

[3] Liu, J., Dong, S., Zhu, L., Shi, S., Wang, J. and Fu, L. (2022) Preparation, Luminescence and Potential Application of Rare Earth Sm^{3+}-Doped Fluorphlogopite Phos-

phors. *Journal of Luminescence*, **244**, Article ID: 118685. https://doi.org/10.1016/j.jlumin.2021.118685

[4] Ishii, M., Komuro, S. and Morikawa, T. (2003) Study on Atomic Coordination Around Er Doped into Anatase- and Rutile-TiO_2: Er-O Clustering Dependent on the Host Crystal Phase. *Journal of Applied Physics*, **94**, 3823-3827. https://doi.org/10.1063/1.1602567

[5] Batra, A., Showe, A., Sampson, J., Kassu, A., Curley, M. and Arun, K. (2018) Fabrication and Optical Characterization of Polyvinylidene Fluoride/Neodymium Oxide Nanocomposite Films. *Open Access Library Journal*, **6**, e5979. https://doi.org/10.4236/oalib.1105979

[6] Vakhidovich, U., Gruber, J.B. and Burdick, G.W. (2012) Magnetooptical Spectroscopy of the Rare-Earth Compounds: Development and Application. Chapter 1 Magnetism of the Rare-Earth Ions in Crystals. Scientific Research Publishing, Wuhan, 9-35.

[7] Judd, B.R. (1962) Optical Absorption Intensities of Rare-Earth Ions. *Physical Review*, **127**, 750-761. https://doi.org/10.1103/PhysRev.127.750

[8] Ishii, M., Towlson, B., Poolton, N., Harako, S., Zhao, X., Komuro, S. and Hamilton, B. (2012) Effects of Oxidization and Deoxidization on Charge-Propagation Dynamics in Rare-Earth-Doped Titanium Dioxide with Room-Temperature Luminescence. *Journal of Applied Physics*, **111**, Article ID: 053514. https://doi.org/10.1063/1.3691241

[9] Sogabe, T., Hung, C.-Y., Tamaki, R., Tomić, S., Yamaguchi, K., Ekins-Daukes, N. and Okada, Y. (2021) Experimental Demonstration of Energy-Transfer Ratchet Intermediate-Band Solar Cell. *Communications Physics*, **4**, Article No. 38. https://doi.org/10.1038/s42005-021-00543-1

[10] Wu, Z., Fan, Y., Hu, R., Ren, W., Li, Y., Wang, Q., Qiu, J., Yang, Z. and Song, Z. (2022) Locking Energy Transfer of Rare Earth Ions via an "Electron Jam" Caused by Vertical Photocarrier Separation of a Layered Semiconductor. *The Journal of Physical Chemistry C*, **126**, 3502-3511. https://doi.org/10.1021/acs.jpcc.1c09322

[11] Fujii, M., Hayashi, S. and Yamamoto, K. (1998) Excitation of Intra-4*f* Shell Luminescence of Yb^{3+} by Energy Transfer from Si Nanocrystals. *Applied Physics Letters*, **73**, 3108-3110. https://doi.org/10.1063/1.122688

[12] Schweizer, T., Möbert, P.E.-A., Hector, J.R., Hewak, D.W., Brocklesby, W.S., Payne, D.N. and Huber, G.H. (1998) Optical Measurement of Narrow Band Rare-Earth 4*f* Levels with Energies Greater than the Band Gap of the Host. *Physical Review Letters*, **80**, 1537-1540. https://doi.org/10.1103/PhysRevLett.80.1537

[13] Hoang, K. (2021) Tuning the Valence and Concentration of Europium and Luminescence Centers in GaN through Co-Doping and Defect Association. *Physical Review Materials*, **5**, Article ID: 034601.

[14] Zhou, J., Zheng, G., Liu, X., Dong, G. and Qiu, J. (2021) Defect Engineering in Lanthanide Doped Luminescent Materials. *Coordination Chemistry Reviews*, **448**, Article ID: 214178. https://doi.org/10.1016/j.ccr.2021.214178

[15] Sah, C.T., Forbes, L., Rosier, L.L. and Tasch, A.F. (1970) Thermal and Optical Emission and Capture Rates and Cross Sections of Electrons and Holes at Imperfection Centers in Semiconductors from Photo and Dark Junction Current and Capacitance Experiments. *Solid-State Electronics*, **13**, 759-788. https://doi.org/10.1016/0038-1101(70)90064-X

[16] Lang, D.J. (1974) Deep-Level Transient Spectroscopy: A New Method to Characterize Traps in Semiconductors. *Journal of Applied Physics*, **45**, 3023-3032.

https://doi.org/10.1063/1.1663719

[17] Lang, D.J. (2007) Recalling the Origins of DLTS. *Physica B*: *Condensed Matter*, **401-402**, 7-9. https://doi.org/10.1016/j.physb.2007.08.102

[18] Peaker, A.R., Markevich, V.P. and Coutinho, J. (2018) Tutorial: Junction Spectroscopy Techniques and Deep-Level Defects in Semiconductors. *Journal of Applied Physics*, **23**, Article ID: 161559. https://doi.org/10.1063/1.5011327

[19] Asalzadeha, S. and Yasserian, K. (2019) The Effect of Various Annealing Cooling Rates on Electrical and Morphological Properties of TiO_2 Thin Films. *Semiconductors*, **53**, 1603-1607. https://doi.org/10.1134/S1063782619160036

[20] Jing, F., Harako, S., Komuro, S. and Zhao, X. (2009) Luminescence Properties of Sm^{3+}-Doped TiO_2 Thin Films Prepared by Laser Ablation. *Journal of Physics D*: *Applied Physics*, **42**, Article ID: 085109. https://doi.org/10.1088/0022-3727/42/8/085109

[21] Kim, M., Osone, S., Kim, T., Higashi, H. and Seto, T. (2017) Synthesis of Nanoparticles by Laser Ablation: A Review. *KONA Powder and Particle Journal*, **34**, 80-90. https://doi.org/10.14356/kona.2017009

[22] Bauer, W. and Perram, G. (2018) Laser Ablated Ti Velocity Distribution Dynamics. *Journal of the Optical Society of America B*, **35**, B27-B37. https://doi.org/10.1364/JOSAB.35.000B27

[23] Murakami, Y., Tue, P.T., Tsukada, H., Li, J. and Shimoda, T. (2013) Preparation of Ruthenium Metal and Ruthenium Oxide Thin Films by a Low-Temperature Solution Process. *Proceedings of the* 20*th International Display Workshops* (*IDW*'13), **20**, 1573-1576.

[24] Miyagi, T., Kamei, M., Mitsuhashi, T. and Yamazaki, A. (2003) Superior Schottky Electrode of Ruo_2 for Deep Level Transient Spectroscopy on Anatase Tio_2. *Applied Physics Letters*, **83**, 1782-1784. https://doi.org/10.1063/1.1606869

[25] Ngbiche, D., Nkrumah, I., Ampong, F., Paal, M., Nkum, R. and Boakye, F. (2019) Optical and Structural Properties of Chemical Bath Deposited Cadmium Sulphur Selenide ($CdS_{1-x}Se_x$ ($0 \le x \le 1$)) Thin Films. *Open Journal of Applied Sciences*, **9**, 785-798. https://doi.org/10.4236/ojapps.2019.911064

[26] Patil1, V., Pawar, S., Chougule, M., Godse, P., Sakhare, R., Sen, S. and Joshi, P. (2011) Effect of Annealing on Structural, Morphological, Electrical and Optical Studies of Nickel Oxide Thin Films. *Journal of Surface Engineered Materials and Advanced Technology*, **1**, 35-41. https://doi.org/10.4236/jsemat.2011.12006

[27] Haider, A.J., Jameel, Z.N. and Al-Hussaini, I.H.M. (2019) Review on: Titanium Dioxide Applications. *Energy Procedia*, **157**, 17-29. https://doi.org/10.1016/j.egypro.2018.11.159

[28] us Saqib, N., Adnan, R. and Shah, I. (2016) A Mini-Review on Rare Earth Metal-Doped TiO_2 for Photocatalytic Remediation of Wastewater. *Environmental Science and Pollution Research*, **23**, 15941-15951. https://doi.org/10.1007/s11356-016-6984-7

[29] Cerchez, M., Langer, H., El Achhab, M., Heinzel, T., Ostermann, D., Lüder, H. and Degenhardt, J. (2013) Dynamics of Hydrogen Sensing with Pt/TiO_2 Schottky Diodes. *Applied Physics Letters*, **103**, Article ID: 033522. https://doi.org/10.1063/1.4816265

[30] Komuro, S., Katsumata, T., Kokai, H., Morikawa, T. and Zhao, X. (2002) Change in Photoluminescence from Er-Doped TiO_2 Thin Films Induced by Optically Assisted Reduction. *Applied Physics Letters*, **81**, 4733-4735. https://doi.org/10.1063/1.1530733